

Circ-100290 Regulates Autophagy-Mediated Angiogenesis of Human Umbilical Vein Endothelial Cells Induced by Conditioned Medium of Human Amniotic Mesenchymal Stem Cells

Leiting Yang^{1,2,†}, Han Yan^{1,3,†}, Yi Liang^{1,2,4}, Dian Sun^{1,2}, Shijun Lu^{1,2,5}, Zichun Tang^{1,2,5}, Ming Ma^{1,2,6,*}, Ming Shen^{1,2,7,*}

¹Jiangsu Province Key Laboratory of Oral Diseases, Nanjing Medical University, 210029 Nanjing, Jiangsu, China

²Jiangsu Province Engineering Research Center of Stomatological Translational Medicine, Nanjing Medical University, 210029 Nanjing, Jiangsu, China

³Department of Oral and Maxillofacial Surgery, Yangzhou Stomatological Hospital, 225002 Yangzhou, Jiangsu, China

⁴Department of Oral and Maxillofacial Surgery, Nanjing Stomatological Hospital, Medical School of Nanjing University, 210093 Nanjing, Jiangsu, China

⁵Department of Oral and Maxillofacial Surgery, Suzhou Stomatological Hospital, 215005 Suzhou, Jiangsu, China

⁶Endodontic Department, School of Stomatology, Nanjing Medical University, 211166 Nanjing, Jiangsu, China

⁷Department of General Dentistry, Affiliated Hospital of Stomatology, Nanjing Medical University, 211166 Nanjing, Jiangsu, China

*Correspondence: mm04110112@126.com (Ming Ma); shenming@njmu.edu.cn (Ming Shen)

†These authors contributed equally.

Published: 2 June 2023

Background: Conditioned medium (CM) from human amnion-derived mesenchymal stem cells (hAMSCs) exhibits excellent pro-angiogenic capacity, and circ-100290 participates in this process. Autophagy is involved in the relevant mechanisms of angiogenesis, but it is unclear whether autophagy is related to the pro-angiogenesis effect of hAMSCs. This research sought to determine whether autophagy involved in the process of pro-angiogenesis induced by hAMSCs might be regulated by circ-100290.

Methods: Upon treatment with CM from hAMSC or 3-methyladenine (3-MA), autophagosomes in human umbilical vein endothelial cells (HUVECs) were observed by transmission electron microscopy. HUVECs' angiogenic ability was evaluated by *in vitro* assays (transwell, wound healing, tube formation) and an *in vivo* Matrigel plug assay. Specific small interfering RNAs (siRNA) or inhibitors were used to regulate circ-100290 expression. Additionally, western blot and quantitative reverse transcription-polymerase chain reaction (RT-qPCR) were used to evaluate expression of the following indicators: Beclin-1, LC3-II, matrix metalloproteinase 2 (MMP2), MMP9, vascular endothelial growth factor (VEGF)-A, and endothelial nitric oxide synthase (eNOS). **Results:** Incubation with hAMSC-CM increased autophagy, angiogenesis and the expressions of VEGF-A and eNOS in HUVECs, all of which were inhibited by 3-MA. Knocking down circ-100290 in hAMSC-CM-treated HUVECs reduced Beclin-1 expression and inhibited autophagy. This resulted in lower angiogenesis in the Matrigel plug assay showing that reduced angiogenesis occurred after circ-100290 silencing in hAMSC-CM-treated HUVECs.

Conclusions: Circ-100290 promotes autophagy-mediated angiogenesis in hAMSC-CM-treated HUVECs.

Keywords: amnion-derived mesenchymal stem cells; autophagy; angiogenesis; circRNA-100290

Introduction

The provision of essential nutrients, oxygen, and an appropriate microenvironment are important requirements of angiogenesis when treating ischemic diseases (e.g., stroke) and improving tissue regeneration (e.g., bone regeneration) [1,2]. Pro-angiogenesis mechanisms are critical for the recovery processes of ischemic stroke [3]. Recently, associations between osteogenesis and angiogenesis during bone regeneration have been identified, especially at the initial stages [4,5]. Thus, improving angiogenesis may enhance stroke recovery and bone regeneration, as the ev-

idence now suggests that mesenchymal stem cells (MSCs) may also improve therapeutic angiogenesis [6,7]. A recent study also reported that MSCs induced tube formation and enhanced endothelial cell proliferation via paracrine mechanisms [8]. Additionally, in a post-infarction model, a MSC-conditioned medium enhanced angiogenesis actions [9]. In particular, human amnion-derived MSCs (hAMSCs) isolated from abandoned human full-term placentas not only have high pro-angiogenic potential, but also have other advantages that include weaker immunogenicity, ease of acquisition, lack of ethical issues, amplification *in vitro* and extensive sources [10–12]. We previously reported that

hAMSCs promote osteogenesis in an animal model via enhancing angiogenesis [10].

Autophagy is a complex phenomenon in which cellular homeostasis is maintained by encapsulating damaged proteins or organelles into a double-membrane vesicle called the autophagosome. Cargoes in the autophagosome are degraded after fusion with the lysosome, and the resultant products are used as energy sources and synthesis materials in cells [13–15]. Previously, autophagy was implicated in endothelial cell angiogenesis [16,17]. Upon activation of autophagy, oxidative stress was suppressed [18], and low oxidative stress levels benefited angiogenesis [19]. However, it is unclear whether autophagy is implicated in the pro-angiogenic effects of human umbilical vein endothelial cells (HUVECs) when cells are induced by hAMSCs.

Circular RNAs (circRNAs), endogenous noncoding RNAs generated via back-splicing, were previously hypothesized to be transcription byproducts with no biological function [20]. However, recent studies have suggested that circRNAs exert important angiogenesis functions in endothelial cells [21,22]. A previous study investigated the role of circ-100290 in pro-angiogenesis in HUVECs induced by hAMSCs [23]. Furthermore, circ-100290 sponged miR-4b to activate the Wnt/ β -catenin signal pathway, thereby inhibiting apoptosis in colorectal cancer cells [24]. Wnt/ β -catenin is a vital pathway that regulates autophagy and apoptosis [25]. However, it is unclear whether circ-100290 plays a part in the regulatory mechanism of autophagy. In this study, we found that circ-100290 positively regulated HUVEC angiogenesis by increasing autophagy of HUVEC when the cells were treated with hAMSC-conditioned medium (hAMSC-CM). The reporting in this article is in accordance with the ARRIVE reporting checklist (<https://atm.amegroups.com/article/view/10.21037/atm-23-613/rc>).

Methods

Isolation and Culture of hAMSC

The isolation and identification of hAMSC were performed according to previous studies [10,26]. Three female donors with average age 25.3 years (range 24–27 years) were recruited from the Obstetrics Department of Nanjing Maternal and Affiliated Child Health Hospital (enrolled between February 2018 and March 2018) to provide hAMSCs. Briefly, the amnions were separated and cut into pieces sized around 2×2 cm and then digested by 2.4 U/mL dispase (Roche, Mannheim, Germany) for 7 minutes at 37 °C, and then digested by 0.75 mg/mL collagenase (Roche, Mannheim, Germany) and 20 μ g/mL DNase (Roche, Mannheim, Germany) for 3 hours at 37 °C. Digestive fluid was subjected to filtration with a 100 μ m cell strainer for collecting hAMSCs. Then the growth of hAMSCs was supported using α -Minimum Essential

Medium (α -MEM; Gibco, Grand Island, NY, USA) containing 100 U/L penicillin, 100 mg/L streptomycin, and 10% fetal bovine serum (FBS; Gibco, Grand Island, NY, USA). Passage 3–5 cells were used for studies. Dulbecco's Modified Eagle Medium (DMEM, Gibco, Grand Island, NY, USA) containing 100 mg/L streptomycin, 100 U/L penicillin, and 10% FBS was used for supporting the growth of HUVECs (China Infrastructure of Cell Line Resources, Beijing, China). HUVECs were authenticated by STR genotyping. A mycoplasma test was done on HUVECs and hAMSC by polymerase chain reaction (PCR) to confirm that they were not contaminated.

hAMSC-Conditioned Medium (hAMSC-CM) Collection

At 70–80% confluence, hAMSCs were rinsed three times with phosphate-buffered saline (PBS). Then a 1-day incubation of the cells was conducted with serum-free α -MEM and serum-free DMEM, both containing penicillin and streptomycin (15 mL) [26]. The medium was removed, followed by 5-minute centrifugation ($1500 \times g$, 4 °C), 3-minute centrifugation ($3000 \times g$, 4 °C), and then filtration through a 0.45- μ m membrane (Merck Millipore, Darmstadt, Germany). The hAMSC-CM was frozen at -80 °C. During hAMSC-CM harvesting, hAMSCs were cultured separately in triplicate. As previously identified [27], 80% (v/v) hAMSC-CM in fresh medium (hAMSC-CM or CM) was used for all studies unless otherwise indicated. Serum-free medium (not used for hAMSC incubation) served as control media.

Endothelial Cell Proliferation

A Cell Counting Kit-8 (CCK8) kit (Dojindo, Kumamoto, Japan) was used to measure proliferation of HUVECs, following kit protocols. HUVECs in DMEM containing 10% FBS were plated into 96-well plates (1×10^3 cells/well). Cells were incubated at 37 °C overnight, and cultured in DMEM containing 2% FBS for 1 day. Then, HUVECs were co-cultured with CM supplemented with 0, 1, 5, 10, or 20 mM 3-methyladenine (3-MA; Sigma-Aldrich, St. Louis, MO, USA). To assess HUVEC proliferation, a microplate reader (Bio-Tek, Winooski, VT, USA) provided detection of the optical density at 450 nm. Each experiment was repeated independently three times.

Tube Formation

After coating of 96-well plates with reduced Matrigel growth factor (BD Biosciences, Franklin Lakes, NJ, USA), HUVECs (3×10^3 cells/well) were added to the plates [26]. Five random fields were processed by optical microscopy (Zeiss, Thornwood, NY, USA) after 6 hours of incubation with control medium or hAMSC-CM (both containing 1% FBS). The total tube length was quantified using ImageJ software (Version 1.40, National Institute of Health, Bethesda, MD, USA).

Wound Healing Assay

Cells in the logarithmic phase were seeded into 6-well plates to generate confluent HUVEC monolayers. Once monolayers were established, a straight line was drawn across the monolayer using an autoclaved pipette tip. The cell debris was washed away three times with PBS. Control medium or CM containing 2% FBS was then added, respectively. Images were obtained at 0 and 16 hours. The gap distances in images were analyzed using ImageJ software. Five random gap locations were measured per group.

Transwell Migration Assay

Migration of HUVECs was detected utilizing 24-well transwell inserts (8 nm pores, 6.5 mm diameter; Corning, Inc., NY, USA). After resuspension of HUVECs in logarithmic phase using 200 μ L control medium (not containing FBS), 1.5×10^4 HUVECs was added to each well of the upper chambers. Lower chambers contained 600 μ L control medium or CM (containing 10% FBS). After 12 hours, fixation with 4% paraformaldehyde and staining with crystal violet were performed for HUVECs on lower filter surfaces. Cells from five random fields were counted using digital microscopy (Carl Zeiss Microscopy GmbH, Oberkochen, Germany). All assays were independently performed three times.

RNA Interference and Transfection

RiboBio (Guangzhou, China) provided three circ-100290-targeted small interfering RNAs (siRNAs) and corresponding siRNA negative control (si-NC). The siRNAs were named si-1, si-2, and si-3. HUVECs entering the log phase were digested and resuspended. On completion of cell seeding in 6-well plates, the cells were observed until 80–90% confluence was reached. Cell transfection was subsequently conducted in line with the instructions of Lipofectamine 2000 (Invitrogen, Waltham, MA, USA). Quantitative PCR (qPCR) and western blot were used to measure Beclin-1 expression after two days of transfection. The sequences of quantitative real-time PCR (RT-qPCR) primers, siRNAs, and si-NC are presented (**Supplementary Table 1**).

Western Blot

The culture medium was removed when HUVEC confluence reached 80%, followed by washing with cold PBS (4 °C) three times. The cell proteins were isolated using 300 μ L radioimmunoprecipitation assay (RIPA) protein extraction buffer. The next step was a 30-minute lysis on ice and a 15-minute centrifugation (12,000 \times g, 4 °C) of the lysate. Bicinchoninic acid (BCA) assays were carried out to identify protein concentrations. Separation of the quantified samples was then achieved by sodium dodecyl sulfate-polyacrylamide gel electrophoresis (SDS-PAGE). After protein transfer to polyvinylidene

fluoride (PVDF) membranes (Merck Millipore), incubation of membranes and the following primary antibodies was performed: vascular endothelial growth factor-A (VEGF-A) (Abcam, Cambridge, UK; ab171828; 1:200 dilution), endothelial nitric oxide synthase (eNOS) (Cell Signaling Technology (CST), Danvers, MA, USA; 9586; 1:500 dilution), Beclin-1 (Abcam, ab210498; 1:1000 dilution), matrix metalloproteinase 2 (MMP2; Abcam, ab97779; 1:1000 dilution), MMP9 (Abcam, ab76003; 1:1000 dilution), and β -actin (CST; 4970; 1:1000 dilution). The culture conditions were different, with one hour at room temperature (RT) for VEGF-A and overnight incubation at 4 °C for eNOS, Beclin-1 and β -actin. 0.1% Tween-20 in Tris-buffered saline was used to rinse membranes after primary antibody incubation. Next, a one hour incubation with secondary horseradish peroxidase antibody (CST; 80403; 1:10000 dilution) was carried out at RT. Finally, enhanced chemiluminescence was dropped into the membranes to visualize protein bands. ImageJ software was responsible for analyzing the gray level of protein bands. Calculation and normalization of the relative protein expression were done with β -actin as an internal reference.

Oxidative Stress-Related Biomarkers

From extracted supernatants, oxidative stress-related biomarkers were assayed using commercial kits (Beyotime, Shanghai, China). The kits used included a Lipid Peroxidation MDA Assay Kit for measurement of malondialdehyde (MDA) levels at 532 nm, a Total Superoxide Dismutase Assay Kit for detection of superoxide dismutase (SOD) activity at 550 nm, and a Glutathione Peroxidase Assay Kit for determination of glutathione peroxidase (GSH-Px) activity. A microplate reader (Bio-Tek, Winooski, VT, USA) was used for all assays.

Quantitative Real-Time PCR (RT-qPCR)

Following RNA isolation using TRIzol reagent (Invitrogen, USA), the RNA quantity and quality levels were detected by a Nanodrop 2000 spectrophotometer (Thermo Fisher Scientific, Waltham, MA, USA). With a Prime Script RT Master Mix (Takara Bio, Shiga, Japan), reverse transcription was carried out to achieve the conversion from RNA (1 μ g) to complementary DNA (cDNA). Expression of RNA was identified by ABI 7500 PCR system (Thermo Fisher Scientific, Waltham, MA, USA) in line with the instructions of SYBR Green master mix (Takara Bio, Japan). The $2^{-\Delta\Delta C_t}$ method was used as a quantification strategy for relative RNA fold-change levels. Glyceraldehyde 3-phosphate dehydrogenase (GAPDH) served as an internal control. RT-qPCR was performed three times. The primer sequences are shown in **Supplementary Table 1**.

eNOS Production

3-amino-4-aminomethyl-2i, 7'-difluorescein, diacetate (DAF-FM DA) (Beyotime, China), a specific NO flu-

orescent stain, was used to evaluate NO production [24]. Briefly, we washed the cells with PBS three times after 40-minute incubation of HUVECs and 5 nM DAF-FM DA at 37 °C. Dynamic fluorescence intensity levels at 495 nm were quantified on a SPECTRONIC™ 200 spectrophotometer (Thermo Fisher Scientific, Waltham, MA, USA). Images were processed in ImageJ Software. DAF-FM fluorescence intensity was normalized to fluorescence areas, then to respective controls.

Transmission Electron Microscopy (TEM)

Fixation steps of HUVECs included 2-hour fixation in 0.1 M sodium dimetharsenate containing 2.5% glutaraldehyde, followed by 1.5-hour fixation in 1% osmium tetroxide. After washing with PBS, cells were incubated with 3% uranyl acetate for one hour. The cells, after washing again with PBS, were subjected to dehydration using alcohol and embedding using Epon-Araldite resin (Canemco, Quebec, CA). Ultrathin sections were obtained using an ultramicrotome (Reichert-Jung, Depew, NY, USA). An EM420 electron microscope (Philips, Oxford, UK) provided three independent observations of the ultrathin sections stained in 0.3% lead citrate. Statistical analysis was performed for the number of autophagic vacuoles per cell.

Matrigel Plug Assays

BALB/c athymic nude mice (body-weight: 20.2 g \pm 3.3 g, 6-week-old, female) were obtained from Model Animal Research Center of Nanjing University (Nanjing, China). All animals were housed in an animal room (12 h light/dark cycles, temperature: 22 \pm 2 °C, humidity: 50 \pm 20%) with free access to food (SZS9126, Xietong Pharmaceutical, China) and distilled water. Mice were placed in plastic cage (37 \pm 29 \pm 12 cm) (3 mice/cage). All mice were subcutaneously injected with HUVECs (3×10^5) in a 100 μ L solution containing 50% Matrigel (354277, Corning Costa Co., MA, USA) into the right flank. Seventy plugs were collected and photographed after 7 days. The degree of vascularization of half the plugs was evaluated by determining hemoglobin (Hb) content. Then the remaining plugs were immunohistochemically stained for CD31 (CST; Cat. No. 77699; 1:100 dilution).

Immunohistochemistry

Following fixation of the plugs with 10% paraformaldehyde, they were embedded in paraffin. After cutting the embedded samples into 5 μ m sections, dewaxing them, and affixing them to microscope slides, the sections were boiled in 100 mM sodium citrate solution for 15 min to block endogenous peroxidase activity. They were next exposed to 3% hydrogen peroxide for 10 minutes before incubation with primary antibody (CD31, CST; Cat. No. 77699; 1:100 dilution) overnight at 4 °C. Next, slices were subjected to secondary antibody incubation (CST; 80403; 1:1000 dilution) at RT for 1

hour and 3,3'-diaminobenzidine tetrahydrochloride (DAB) reagent (Beyotime, China) for 10 min. Finally, nuclei were stained with Mayer's hematoxylin (Solarbio Life Sciences, Beijing, China). ImageJ software was used to analyze the positive staining area of CD31.

Statistical Analysis

All studies were independently performed three times, and image analyses were processed blindly. The data are presented as Mean \pm Standard Error of Mean (SEM). SPSS 20.0 (Abbott Laboratories, Chicago, IL, USA) was used for data processing. We performed one-way analysis of variance for comparing differences, followed by Tukey's post-hoc tests to determine significant difference between groups. The statistical significance was expressed as $p < 0.05$.

Results

hAMSC-CM Enhances Autophagy-Regulated Angiogenesis in HUVECs

Previous study confirmed that hAMSC-CM promoted angiogenesis in HUVECs [23]. However, it was unclear whether autophagy was involved. Here, we used 3-MA (an autophagy inhibitor) to investigate the role of autophagy. First, with CCK-8, the effect of intervention time and concentration of 3-MA on HUVECs was evaluated. 10 and 20 mM 3-MA treatment decreased the survival rate of HUVECs ($p < 0.05$), and the survival rate gradually declined with the duration of intervention (Fig. 1A). But there was no significant effect on cell survival rate after 1 and 5 mM 3-MA treatment ($p > 0.05$). Meanwhile, we investigated the effect of 5 mM 3-MA on autophagy of HUVECs by western blot. Significant declines of Beclin-1 protein expression and LC3-II/LC3-I ratio occurred after 3-72h incubation of 5 mM 3-MA compared with 0 h ($p < 0.05$, Fig. 1B–C), suggesting inhibition of HUVEC autophagy after 5 mM 3-MA incubation.

Next, HUVECs were treated with control medium (Ctrl group), hAMSC-CM (CM group) and hAMSC-CM + 5 mM 3-MA (CM + 3-MA group). Beclin-1 expression and LC3-II/LC3-I ratio in CM group were markedly higher than those in Ctrl group, but lower than those in CM + 3-MA group ($p < 0.05$, Fig. 1D–E). Autophagy levels in the three groups were also examined via TEM. Autophagosome number in HUVECs showed a rise in CM group in comparison with Ctrl group ($p < 0.05$). The autophagosome number in CM + 3-MA group was lower than in the CM group ($p < 0.05$, Fig. 1F). It suggested that hAMSC-CM stimulated autophagy in HUVECs. In addition, we investigated the changes of oxidative stress markers (MDA, SOD, and GSH-Px) levels in each group. hAMSC-CM significantly decreased MDA level ($p < 0.05$), raise SOD and GSH-Px levels in HUVECs ($p < 0.05$). 3-MA reversed the decrease of MDA and the increase of SOD and GSH-Px in-

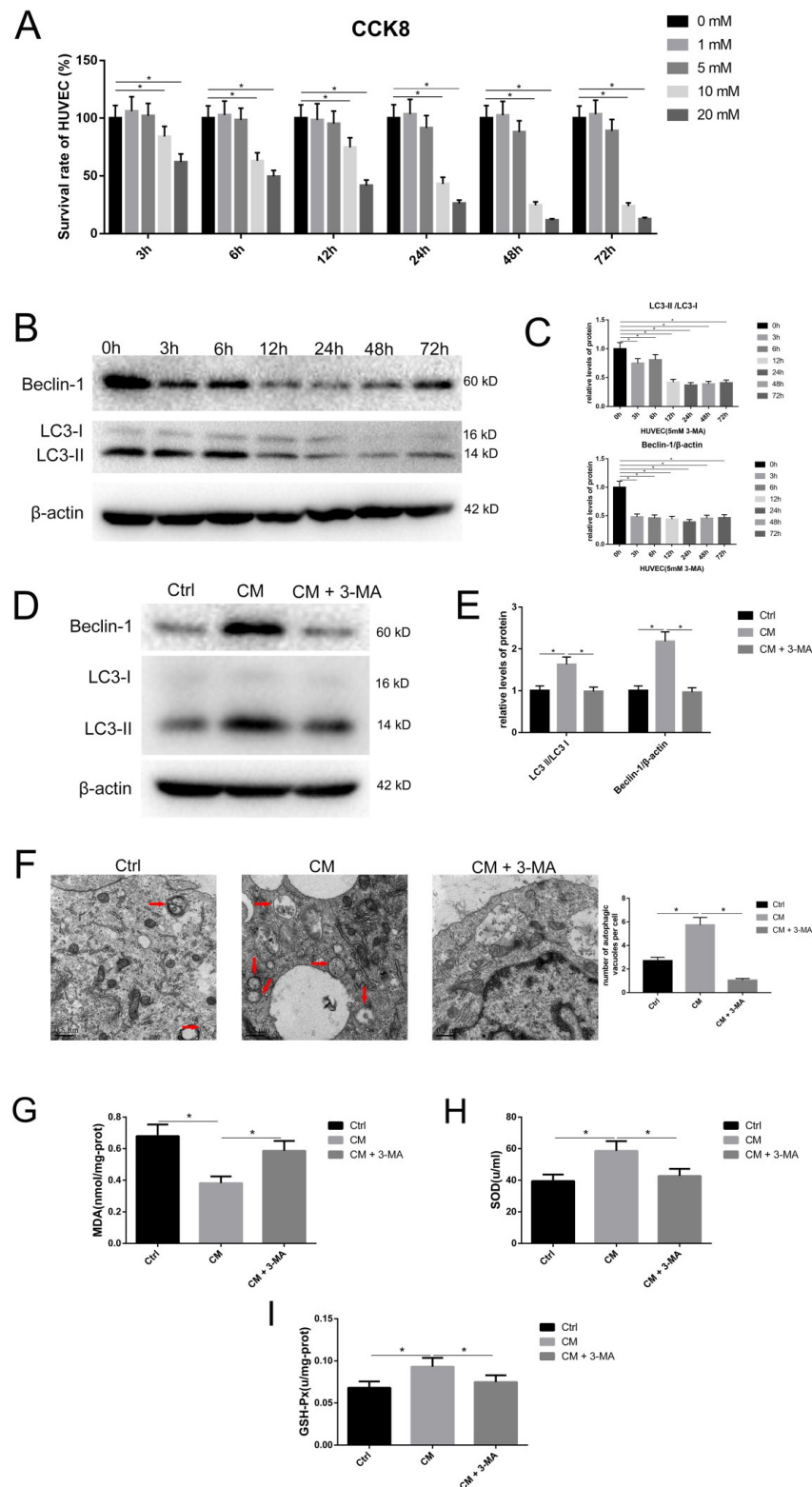


Fig. 1. hAMSC-CM enhances autophagy in HUVECs. (A) The survival rate of HUVECs under different concentrations of 3-MA treatment was studied using the CCK8 assay. $N = 3$. (B,C) Western blot assay of LC3-II, LC3-I and Beclin-1 protein expression in HUVECs treated with 5 mM 3-MA at different time points. $N = 3$. (D,E) Western blot assay of LC3-II, LC3-I and Beclin-1 proteins expression in HUVECs in each group. $N = 3$. (F) TEM scanning was used to observe autophagy in HUVECs. Arrowheads indicate autophagosomes. Scale bar: 0.5 μ m. (G–I) Levels of MDA, SOD, and GSH-Px in HUVECs were determined, which was rescued by adding 5 mM 3-MA. $N = 3$. * $p < 0.05$. Ctrl, control medium; CM, hAMSC-CM; 3-MA, 3-methyladenine; TEM, transmission electron microscopy; HUVEC, human umbilical vein endothelial cells.

duced by hAMSC-CM ($p < 0.05$, Fig. 1G–I), suggesting that hAMSC-CM suppressed oxidative stress levels.

Since autophagy could affect angiogenesis, we evaluated the angiogenic ability of HUVECs. Based on transwell migration and wound healing assays, hAMSC-CM improved migration of HUVECs. The migration of HUVECs was reduced in the CM + 3-MA group compared to the CM group ($p < 0.05$, Fig. 2A–B). hAMSC-CM increased the protein and mRNA expression of MMP2 and MMP9 in comparison with the Ctrl group ($p < 0.05$). The protein and mRNA expression of MMP2 and MMP9 was decreased after CM + 3-MA treatment compared to CM ($p < 0.05$, Fig. 2C). Furthermore, tube formation assays showed that hAMSC-CM resulted in enhanced HUVEC angiogenesis, while hAMSC-CM + 3-MA reversed this enhancement ($p < 0.05$, Fig. 2D). Next, we examined the expression of angiogenesis-related genes. VEGF-A and eNOS mRNA expression were up-regulated by hAMSC-CM but down-regulated by CM + 3-MA ($p < 0.05$, Fig. 2E). Western blot results of both VEGF-A and eNOS protein expression displayed a similar tendency with RT-qPCR (Fig. 2F). Finally, we evaluated eNOS activity by detecting DAF-FM DA fluorescence. hAMSC-CM caused an increase in DAF-FM DA fluorescence, but 3-MA treatment reversed the increase of DAF-FM DA fluorescence induced by hAMSC-CM ($p < 0.05$, Fig. 2G). Collectively, hAMSC-CM enhanced HUVEC autophagy and upregulated VEGF-A, eNOS, MMP2, and MMP9 levels, which may have promoted HUVEC angiogenesis.

Circ-100290 Promotes Autophagy-Regulated HUVEC Angiogenesis in the Presence of hAMSC-CM

Beclin-1 is a key autophagy protein. Its expression levels in HUVECs were increased after the incubation of hAMSC-CM, but 3-MA reversed the increase in expression induced by hAMSC-CM. CircRNAs may regulate autophagy in cancer cells [28,29]. We previously reported increased circ-100290 levels, suggesting that circ-100290 may be involved in angiogenesis in hAMSC-CM-treated HUVECs [23]. We investigated whether autophagy is associated with the participation of circ-100290 in HUVEC angiogenesis. A moderately effective siRNA (si-1) from 3 circ-100290-specially targeted siRNAs was selected for further studies [23]. Compared with si-NC, the knock down of circ-100290 markedly decreased the mRNA and protein expression of Beclin-1 in HUVECs ($p < 0.05$, Fig. 3A,B). TEM results demonstrated that knocking down circ-100290 significantly reduced autophagosomes in HUVECs compared with si-NC (Fig. 3C). These results suggest that the knock down of circ-100290 inhibited the autophagy in HUVECs.

Next, we investigated angiogenesis in HUVECs after circ-100290 downregulation. According to transwell and wound healing assays, down-regulation of circ-100290 reduced the migration of HUVECs ($p < 0.05$,

Fig. 3D,E). Tube formation assays confirmed inhibition of HUVEC angiogenesis after the down-regulation of circ-100290 (Fig. 3F). Thus, circ-100290 may be involved in autophagy-promoted angiogenesis on HUVECs incubated with hAMSC-CM.

Circ-100290 Regulates Angiogenesis of HUVECs Plus hAMSC-CM by Promoting Autophagy

We performed *in vivo* Matrigel plug assays to examine the effect of autophagy on pro-angiogenic hAMSC-CM activity in HUVECs. We observed enhanced angiogenesis in the CM group compared with the Ctrl group ($p < 0.05$), while this process was inhibited in CM + 3-MA group (Fig. 4A). Similar results were observed with CD31 staining by immunohistochemistry (Fig. 4B). We also performed *in vivo* Matrigel plug assays to determine whether the circ-100290 promoted HUVEC angiogenesis. The cells were subjected to hAMSC-CM using the following experimental groups: Ctrl, blank+CM, si-1+CM, and si-NC+CM. The results showed a marked rise in angiogenesis in the blank+CM group compared to the Ctrl group ($p < 0.05$). In comparison with the si-NC+CM group, angiogenesis was significantly inhibited in the si-1+CM group ($p < 0.05$). However, there was no significant difference in angiogenesis between the blank+CM group and the si-NC+CM group ($p > 0.05$, Fig. 4C). Similar results were found by CD31 staining (Fig. 4D).

Discussion

Autophagy generates necessary molecules and provides energy for basic homeostatic maintenance by digesting protein or organelle cargoes in lysosomes [13,14]. The complex including Beclin-1 mediates the formation of a phagophore. The phagophore then engulfs cytoplasmic materials and finally forms an autophagosome. LC3 is converted to LC3-I and LC3-II (an autophagic vesicle-associated form of LC3) during this process. The autophagosome fuses with lysosomes to further degrade materials to provide molecules and energy for the cell [13,14]. During angiogenesis, autophagy, as a dynamic regulatory mechanism, enables endothelial cells to adjust the energy needs in response to constantly changing environments [17]. Under normal cultivation environment, HUVECs exhibit adaptive autophagy levels. The autophagy of HUVECs is regulated by different cellular stressors, such as oxidative stress, hypoxia, and cytokines [30]. Current evidence now proposes that enhancing autophagy promotes angiogenesis [31]. Here, we reported that hAMSC-CM enhanced autophagy in HUVECs to promote angiogenesis.

Endothelial cell autophagy may be regulated by paracrine mechanisms, which adapt cells to their microenvironment, as observed in some cancers. The tumor microenvironment (TME) usually displays metabolic stress, reduced nutrient supply, and hypoxia-related limited blood

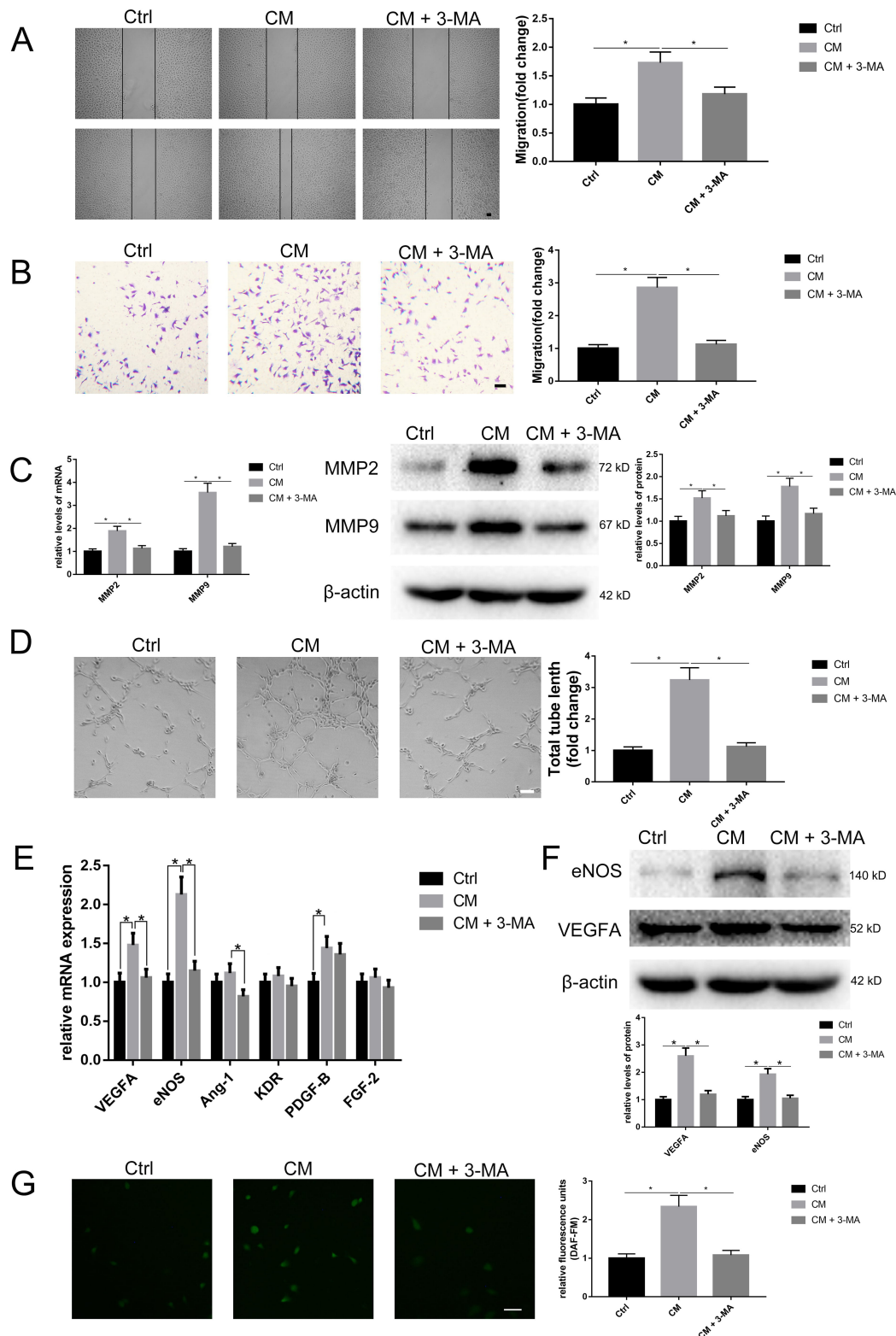


Fig. 2. hAMSC-CM enhances autophagy-regulated angiogenesis of HUVECs. (A,B) Wound healing assays and transwell migration assays were used to examine HUVEC migration. Scale bar: 100 μ m. N = 3. (C) RT-qPCR and western blot assays detected MMP-2 and MMP-9 mRNA and protein expression in HUVECs. N = 3. (D) Tube formation assays evaluated the vessel structure of HUVECs in each group. Scale bar: 100 μ m. N = 3. (E,F) RT-qPCR and western blots measured VEGF-A, eNOS, Ang-1, KDR, PDGF-B and FGF-2 mRNA and protein expression in HUVECs. N = 3. (G) Enzymatic eNOS activity was evaluated by DAF-FM DA. N = 3, Scale bar: 100 μ m. The concentration of 3-MA was 5 mM. * p < 0.05. Ctrl, control medium; CM, hAMSC-CM; 3-MA, 3-methyladenine; TEM, transmission electron microscopy; HUVEC, human umbilical vein endothelial cells.

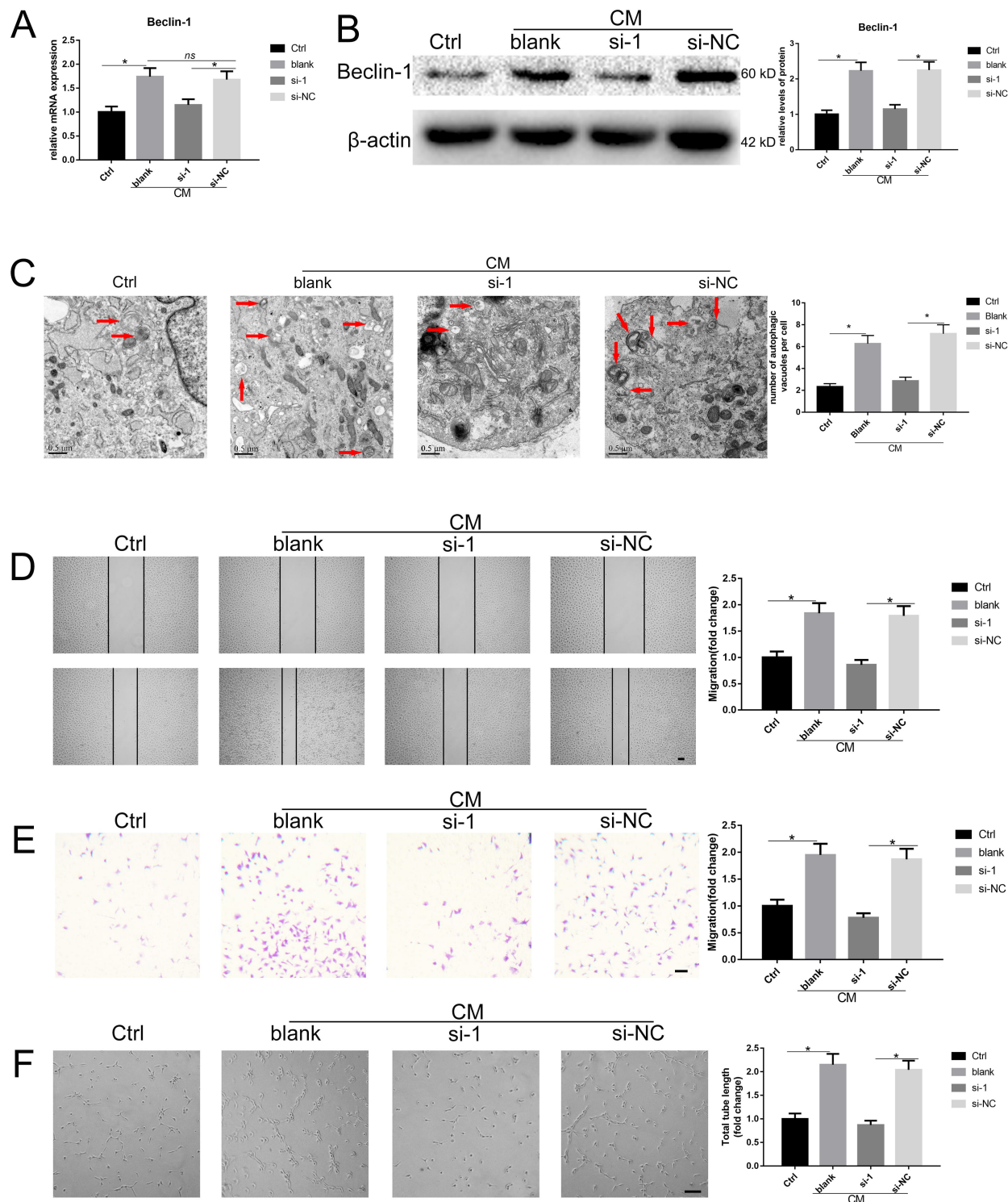


Fig. 3. Circ-100290 promotes autophagy-regulated HUVEC angiogenesis in the presence of hAMSC-CM. (A,B) RT-qPCR and western blot showed downregulated Beclin-1 expression in hAMSC-CM-treated HUVECs after transfection with si-1 (N = 3). (C) TEM scanning and observation showed decreased autophagy in hAMSC-CM-treated HUVECs after transfection with si-1. Arrows indicate autophagosomes. Scale bar: 0.5 μ m. (D,E) Wound healing assay with migration rate calculating and transwell assays with crystal violet staining showed migration of hAMSC-CM-treated HUVECs was inhibited after transfection with si-1. Transwell assays were determined by crystal violet staining. N = 3, Scale bar: 100 μ m. (F) Tube formation assays with vessel structure formation analysis showed that angiogenesis of hAMSC-CM-treated HUVECs was inhibited after transfection with si-1 (N = 3), Scale bar: 100 μ m. * p < 0.05. All data were analyzed using one-way ANOVA followed by Tukey's test. Error bars represent SEM. si-1, si-circ-100290-1; NC, negative control; Ctrl, control medium; CM, hAMSC-CM; TEM, Transmission electron microscopy; HUVECs, human umbilical vein endothelial cells.

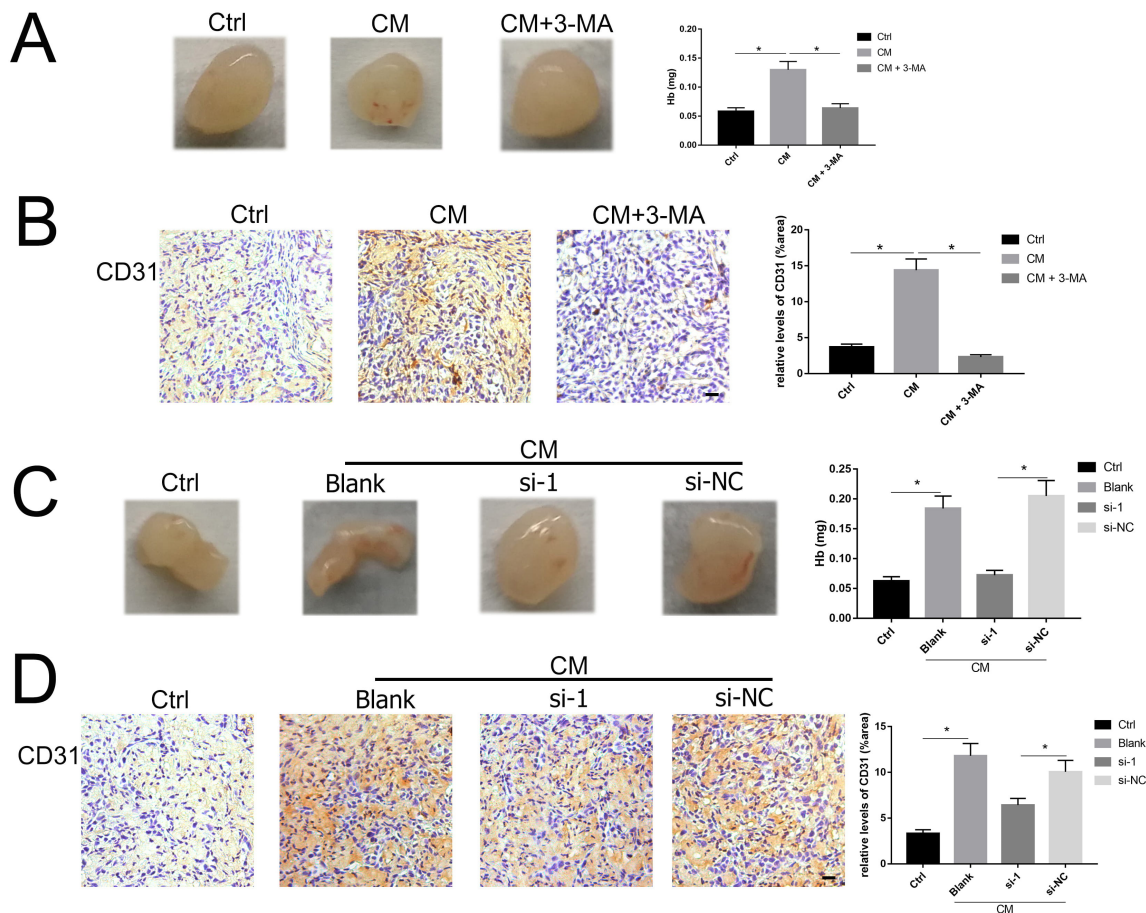


Fig. 4. Circ-100290 regulates angiogenesis of HUVECs plus hAMSC-CM by promoting autophagy. Matrigel plug assay and immunohistochemistry for CD31 evaluated (A,B) the effect of hAMSC-CM or 3-MA on HUVEC angiogenesis or (C,D) knockdown of circ-100290 on HUVEC angiogenesis induced by hAMSC-CM. N = 10, Scale bar: 100 μ m. * p < 0.05. All data were analyzed using one-way ANOVA followed by Tukey's test. Error bars represent SEM. si-1, si-circ-100290-1; NC, negative control; Ctrl, control medium; CM, hAMSC-CM; HUVECs, human umbilical vein endothelial cells.

supply [32]; therefore, the TME may induce autophagy in recruited endothelial cells to form new blood vessels and aid tumor progression [17]. However, it is unclear whether autophagy in endothelial cells induced by stem cells is regulated by paracrine mechanisms. While recent studies have shown that autophagy in periodontal ligament stem cells [33] and MSCs [34] regulates HUVEC angiogenesis, it remains unclear whether HUVEC autophagy is regulated by stem cells. We showed that enhanced autophagy in HUVECs treated with hAMSC-CM promoted angiogenic capacity in these cells.

The effect of cricRNA on autophagy has been reported in some diseases, such as cancer and vascular complications of diabetes [35,36]. CircCCDC66 promoted the migration and invasion of colorectal cancer cells via the miR3140/autophagy pathway in the hypoxic environments [35]. Circ-ADAM9 sponge miR-20a-5p to promote autophagy and apoptosis of diabetic endothelial progenitor cells [36]. Here, we found that knocking down circ-100290 decreased the number of intracellular autophagosomes and

down-regulated Beclin-1 expression. It indicated that circ-100290 promoted cell autophagy in hAMSC-CM induced HUVECs. Recent studies reported that circRNAs binds the response elements of microRNAs to achieve regulation mRNAs expression. Their participation in regulating various biological processes such as autophagy has also been demonstrated [28,37]. Knocking down circRNA-HIPK3 caused upregulation of miR124-3p expression, and accumulation of LC3-II and aggravation of autophagy in non-small cell lung cancer [28]. Previous studies reported that by sponging miR-449a, circ-100290 mediates angiogenesis in HUVECs induced by hAMSC-CM [23]. We speculate that the mechanism of circ-100290 on autophagy may be related to miR-449a, but further investigation is required.

Previous studies have reported the promotion of angiogenesis by circ-100290 in hAMSC-CM-treated HUVECs [23]. Likewise, our study observed that circ-100290 promoted angiogenesis in HUVECs. In addition, we report that autophagy was involved. Furthermore, we report changes in VEGFA and eNOS in autophagy-regulated pro-

angiogenesis in HUVECs induced by hAMSC-CM. However, the exact mechanism of autophagy regulation on oxidative stress, EGFA and eNOS expression in HUVECs remains unknown. Thus, further investigations are required to shed more light on this topic.

Conclusions

This present study demonstrated that circ-100290 was significantly upregulated in HUVECs treated with hAMSC-CM. Circ-100290 increased autophagy levels and promoted angiogenesis by upregulating VEGF-A and eNOS expression in hAMSC-CM-treated HUVECs. Collectively, although we provide new insights into how hAMSCs induce autophagy-regulated angiogenesis, further investigations are needed to identify the molecular mechanisms underpinning increased circ-100290 transcription in HUVECs plus hAMSC-CM.

Availability of Data and Materials

The datasets used in this study are available from the corresponding authors upon reasonable request.

Author Contributions

LTy, HY, MM and MS designed the research study. LTy, HY, MM and MS performed the research. YL, DS, SJL and ZCT provided help and advice on the experiments. YL, DS, SJL and ZCT analyzed the data. All authors contributed to editorial changes in the manuscript. All authors read and approved the final manuscript. All authors have participated sufficiently in the work and agreed to be accountable for all aspects of the work.

Ethics Approval and Consent to Participate

The study was conducted in accordance with the Declaration of Helsinki (as revised in 2013). The study was approved by the Ethics Committee of Nanjing Medical University (No. PJ2013-037-001) and informed consent was obtained from all the patients. Animal studies were approved by Ethics Committee of Nanjing Medical University (approval ID: 2016-640), and in accordance with ethical guidelines. All participants voluntarily participated in this study and provided informed consent.

Acknowledgment

Not applicable.

Funding

This work was supported by A Project Funded by the Priority Academic Program Development of Jiangsu Higher Education Institutions (PAPD, 2018-87), Nature Science Foundation of Jiangsu Province

(BK20221302), Suzhou Science and Technology Development Plan Projects (SYSD2020069, SKJY2021024), and Grant Number JSKLOD-KF-1903 from Jiangsu Province Key Laboratory of Oral Diseases, Nanjing Medical University, China.

Conflict of Interest

All authors have completed the ICMJE uniform disclosure form (*available at: <https://atm.amegroups.com/article/view/10.21037/atm-23-613/coif>*). The authors declare no conflict of interest.

Supplementary Material

Supplementary material associated with this article can be found, in the online version, at <https://doi.org/10.24976/Descov.Med.202335176.39>.

References

- [1] Kohara Y, Kitazawa R, Haraguchi R, Imai Y, Kitazawa S. Macrophages are requisite for angiogenesis of type H vessels during bone regeneration in mice. *Bone*. 2022; 154: 116200.
- [2] Rust R, Grönnert L, Weber RZ, Mulders G, Schwab ME. Refueling the Ischemic CNS: Guidance Molecules for Vascular Repair. *Trends in Neurosciences*. 2019; 42: 644–656.
- [3] Matsushita Y, Nagata M, Kozloff KM, Welch JD, Mizunashi K, Tokavanich N, *et al.* A Wnt-mediated transformation of the bone marrow stromal cell identity orchestrates skeletal regeneration. *Nature Communications*. 2020; 11: 332.
- [4] Diomedea F, Marconi GD, Fonticoli L, Pizzicaniella J, Merciaro I, Bramanti P, *et al.* Functional Relationship between Osteogenesis and Angiogenesis in Tissue Regeneration. *International Journal of Molecular Sciences*. 2020; 21: 3242.
- [5] Wang F, Qian H, Kong L, Wang W, Wang X, Xu Z, *et al.* Accelerated Bone Regeneration by Astragaloside IV through Stimulating the Coupling of Osteogenesis and Angiogenesis. *International Journal of Biological Sciences*. 2021; 17: 1821–1836.
- [6] Bian X, Ma K, Zhang C, Fu X. Therapeutic angiogenesis using stem cell-derived extracellular vesicles: an emerging approach for treatment of ischemic diseases. *Stem Cell Research & Therapy*. 2019; 10: 158.
- [7] Ji X, Yuan X, Ma L, Bi B, Zhu H, Lei Z, *et al.* Mesenchymal stem cell-loaded thermosensitive hydroxypropyl chitin hydrogel combined with a three-dimensional-printed poly(ϵ -caprolactone)/nano-hydroxyapatite scaffold to repair bone defects via osteogenesis, angiogenesis and immunomodulation. *Theranostics*. 2020; 10: 725–740.
- [8] Huang Y, He B, Wang L, Yuan B, Shu H, Zhang F, *et al.* Bone marrow mesenchymal stem cell-derived exosomes promote rotator cuff tendon-bone healing by promoting angiogenesis and regulating M1 macrophages in rats. *Stem Cell Research & Therapy*. 2020; 11: 496.
- [9] Asgari Taei A, Nasoohi S, Hassanzadeh G, Kadivar M, Dargahi L, Farahmandfar M. Enhancement of angiogenesis and neurogenesis by intracerebroventricular injection of secretome from human embryonic stem cell-derived mesenchymal stem cells in ischemic stroke model. *Biomedicine & Pharmacotherapy*. 2021; 140: 111709.
- [10] Jiang F, Ma J, Liang Y, Niu Y, Chen N, Shen M. Amniotic Mesenchymal Stem Cells Can Enhance Angiogenic Capacity

- via MMPs *In Vitro* and *In Vivo*. *BioMed Research International*. 2015; 2015: 324014.
- [11] Wang F, Yao G, Pan S, Mao X, Zhao X, Li C, *et al.* *TIPE2*-modified human amnion-derived mesenchymal stem cells promote the efficacy of allogeneic heart transplantation through inducing immune tolerance. *Journal of Thoracic Disease*. 2021; 13: 5064–5076.
- [12] Wang YH, Yang ZQ, Zhu SF, Gao Y. Comparative study of methotrexate and human umbilical cord mesenchymal stem cell transplantation in the treatment of rheumatoid arthritis. *Journal of Biological Regulators and Homeostatic Agents*. 2018; 32: 599–605.
- [13] Klionsky DJ, Petroni G, Amaravadi RK, Baehrecke EH, Ballabio A, Boya P, *et al.* Autophagy in major human diseases. *The EMBO Journal*. 2021; 40: e108863.
- [14] Li W, He P, Huang Y, Li YF, Lu J, Li M, *et al.* Selective autophagy of intracellular organelles: recent research advances. *Theranostics*. 2021; 11: 222–256.
- [15] Hua Q, Sun L, Li HR, Li HJ, Ma BD, Wang YL. Umbilical cord blood mesenchymal stem cell-derived conditioned medium induces the apoptosis and autophagy of ovarian cancer SKOV3 cells. *Journal of Biological Regulators and Homeostatic Agents*. 2021; 35: 1631–1638.
- [16] Reglero-Real N, Pérez-Gutiérrez L, Nourshargh S. Endothelial cell autophagy keeps neutrophil trafficking under control. *Autophagy*. 2021; 17: 4509–4511.
- [17] Schaaf MB, Houbart D, Meçe O, Agostinis P. Autophagy in endothelial cells and tumor angiogenesis. *Cell Death and Differentiation*. 2019; 26: 665–679.
- [18] Gómez-Puerto MC, Verhagen LP, Braat AK, Lam EWF, Coffey PJ, Lorenowicz MJ. Activation of autophagy by FOXO3 regulates redox homeostasis during osteogenic differentiation. *Autophagy*. 2016; 12: 1804–1816.
- [19] Kang DH, Lee DJ, Lee KW, Park YS, Lee JY, Lee SH, *et al.* Peroxiredoxin II is an essential antioxidant enzyme that prevents the oxidative inactivation of VEGF receptor-2 in vascular endothelial cells. *Molecular Cell*. 2011; 44: 545–558.
- [20] Liu CX, Chen LL. Circular RNAs: Characterization, cellular roles, and applications. *Cell*. 2022; 185: 2016–2034.
- [21] He Q, Zhao L, Liu Y, Liu X, Zheng J, Yu H, *et al.* circ-SHKBP1 Regulates the Angiogenesis of U87 Glioma-Exposed Endothelial Cells through miR-544a/FOXP1 and miR-379/FOXP2 Pathways. *Molecular Therapy. Nucleic Acids*. 2018; 10: 331–348.
- [22] Yu F, Zhang Y, Wang Z, Gong W, Zhang C. Hsa_circ_0030042 regulates abnormal autophagy and protects atherosclerotic plaque stability by targeting eIF4A3. *Theranostics*. 2021; 11: 5404–5417.
- [23] Tang Z, Wu X, Hu L, Xiao Y, Tan J, Zuo S, *et al.* Circ-100290 Positively Regulates Angiogenesis Induced by Conditioned Medium of Human Amnion-Derived Mesenchymal Stem Cells Through miR-449a/eNOS and miR-449a/VEGFA Axes. *International Journal of Biological Sciences*. 2020; 16: 2131–2144.
- [24] Fang G, Ye BL, Hu BR, Ruan XJ, Shi YX. CircRNA_100290 promotes colorectal cancer progression through miR-516b-induced downregulation of FZD4 expression and Wnt/ β -catenin signaling. *Biochemical and Biophysical Research Communications*. 2018; 504: 184–189.
- [25] Lorzadeh S, Kohan L, Ghavami S, Azarpira N. Autophagy and the Wnt signaling pathway: A focus on Wnt/ β -catenin signaling. *Biochimica et Biophysica Acta. Molecular Cell Research*. 2021; 1868: 118926.
- [26] Fan H, Li Y, Liu C, Liu Y, Bai J, Li W. Circular RNA-100290 promotes cell proliferation and inhibits apoptosis in acute myeloid leukemia cells via sponging miR-203. *Biochemical and Biophysical Research Communications*. 2018; 507: 178–184.
- [27] Tang Z, Tan J, Yuan X, Zhou Q, Yuan Z, Chen N, *et al.* Circular RNA-ABC10 promotes angiogenesis induced by conditioned medium from human amnion-derived mesenchymal stem cells via the microRNA-29b-3p/vascular endothelial growth factor A axis. *Experimental and Therapeutic Medicine*. 2020; 20: 2021–2030.
- [28] Chen X, Mao R, Su W, Yang X, Geng Q, Guo C, *et al.* Circular RNA *circHIPK3* modulates autophagy via *MIR124-3p*-STAT3-PRKAA/AMPK α signaling in STK11 mutant lung cancer. *Autophagy*. 2020; 16: 659–671.
- [29] Liang G, Ling Y, Mehrpour M, Saw PE, Liu Z, Tan W, *et al.* Autophagy-associated circRNA *circCDYL* augments autophagy and promotes breast cancer progression. *Molecular Cancer*. 2020; 19: 65.
- [30] Jiang F. Autophagy in vascular endothelial cells. *Clinical and Experimental Pharmacology & Physiology*. 2016; 43: 1021–1028.
- [31] Liang P, Jiang B, Li Y, Liu Z, Zhang P, Zhang M, *et al.* Autophagy promotes angiogenesis via AMPK/Akt/mTOR signaling during the recovery of heat-denatured endothelial cells. *Cell Death & Disease*. 2018; 9: 1152.
- [32] Russell RC, Guan KL. The multifaceted role of autophagy in cancer. *The EMBO Journal*. 2022; 41: e110031.
- [33] Wei W, An Y, An Y, Fei D, Wang Q. Activation of autophagy in periodontal ligament mesenchymal stem cells promotes angiogenesis in periodontitis. *Journal of Periodontology*. 2018; 89: 718–727.
- [34] Lee SG, Joe YA. Autophagy mediates enhancement of proangiogenic activity by hypoxia in mesenchymal stromal/stem cells. *Biochemical and Biophysical Research Communications*. 2018; 501: 941–947.
- [35] Feng J, Li Z, Li L, Xie H, Lu Q, He X. Hypoxia induced circC-CDC66 promotes the tumorigenesis of colorectal cancer via the miR 3140/autophagy pathway. *International Journal of Molecular Medicine*. 2020; 46: 1973–1982.
- [36] Tian D, Xiang Y, Tang Y, Ge Z, Li Q, Zhang Y. Circ-ADAM9 targeting PTEN and ATG7 promotes autophagy and apoptosis of diabetic endothelial progenitor cells by sponging mir-20a-5p. *Cell Death & Disease*. 2020; 11: 526.
- [37] Wang Y, Wang S, Jing H, Zhang T, Song N, Xu S. CircRNA-IGLL1/miR-15a/RNF43 axis mediates ammonia-induced autophagy in broilers jejunum via Wnt/ β -catenin pathway. *Environmental Pollution (Barking, Essex: 1987)*. 2022; 292: 118332.